

Figure 2. Transition states for the addition of the malononitrile radical to ethylene at the UHF/6-31G* level.

The electrophilic radical **4** was generated via chlorine abstraction from chloromalononitrile **7** with tributylstannane at 20 °C in tetrahydrofuran under irradiation (Scheme III). The malononitrile radicals are trapped by styrene **5** and give adduct radicals **6** that yield products **8** after hydrogen abstraction from tributylstannane. In kinetic competition reactions, a 10-fold or greater excess of pairs of styrenes was used. Determination of the product ratio via gas chromatography gives relative rates via pseudo-first-order kinetics.^{2c,7}

Under the conditions of these kinetic experiments, trapping of radical **6** by tributyltin hydride (**6** → **8**) is faster than β -bond cleavage to starting alkene **5** and educt radical **4** (**6** → **4** + **5**).⁸ This was shown in reactions with β -methylstyrene where no isomerization of the cis styrene to the more stable trans compound could be observed.

Thus the results of kinetic experiments favor an unsymmetrical transition state for the addition reaction of electrophilic radicals to alkenes. To provide theoretical evidence for this conclusion, ab initio calculations were carried out for the transition state of the addition of the malononitrile radical **4** to ethylene.⁹ The two transition states **9a** and **9b** are shown in Figure 2. Transition-state structures with angles of attack smaller than 90° could not be found.

The energy difference between reactants and the transition states **9a** and **9b** are 14.5 kcal/mol and 14.3 kcal/mol at the UHF/6-31G*//UHF/6-31G* level.¹⁰ Inclusion of electron correlation effects lowers the energy difference considerably to 8.8 kcal/mol for **9a** and 8.6 kcal/mol for **9b** at the PMP3/6-31G*//UHF/6-31G* level of theory. From Figure 2 it can be seen that the geometries for the two transition states are very similar. A comparison with the transition state **1** shows that the differences in geometry between approach of the electrophilic malononitrile radical **4** and the nucleophilic methyl radical to ethylene are rather small. Only the distance between the reactants is slightly shorter for the malononitrile radical (2.14 Å) as compared to the methyl radical (2.25 Å). The pyramidalization of

the ethylene carbon atom being attacked is 155° for the methyl radical and 150° for the malononitrile radical. These parameters could indicate a somewhat later transition state for the reaction of malononitrile radical **4** with ethylene (transition states **9**) compared to that of addition of methyl radicals (transition state **1**). However, the angle of attack is virtually identical for both systems.

The addition of the electrophilic, heteroatom-based hydroxyl radical to ethylene had been investigated earlier.³ In this transition state the radical approaches the ethylene terminus by an angle of 106.4°. Comparison of the transition structures of nucleophilic radicals^{3,11} to ambiphilic radicals ($\cdot\text{CH}_2\text{CHO}$)¹¹ provides additional computational support for the near constancy of the attack angle α regardless of the nature of the radical.

Acknowledgment. We are grateful to the Swiss National Fonds and the National Science Foundation for financial support and the UCLA Office of Academic Computing for IBM 3090/600J computer time.

Supplementary Material Available: Geometrical data for the transition states **9a** and **9b** (2 pages). Ordering information is given on any current masthead page.

(11) Zipse, H.; Giese, B.; Broeker, J.; Li, Y.; Houk, K. N., unpublished results.

Dependence of Electron Transfer Rates on Donor–Acceptor Angle in Bis-Porphyrin Adducts

Anna Helms, David Heiler, and George McLendon*

Department of Chemistry, University of Rochester
Rochester, New York 14627

Received March 1, 1991

Revised Manuscript Received March 29, 1991

Electron transfer reactions between spatially fixed donor–acceptor pairs play a key role in processes ranging from biology to zoography.¹ When the donor–acceptor separation is much larger than van der Waals contact distance, the electron transfer rate constant, k_{et} , depends markedly on wave function mixing which is characterized by a tunneling matrix element, $|V_{ab}|$:^{1,2} $k_{et} \propto |V_{ab}|^2$. A wide variety of experiments have probed the dependence of rate on donor–acceptor distance, showing that $|V_{ab}| \propto \exp(-\beta R)$.^{1b} Since the interacting wave functions contain not only a radial component but also an angular one, electron transfer rates might also depend markedly on the angle between the donor and acceptor. This question is of some importance in understanding biological electron transfer and has received significant theoretical attention.³ There is some experimental indication of such angular effects on rate in recent studies by Closs and Miller⁴ of bichromophoric molecules.⁴ However, unlike the well-established dependence of rate on distance, no systematic experimental studies of the dependence of rate on donor–acceptor angle are available, although recent studies⁵ by Sessler, Morayuma, and others may bear on this problem. We now report the first such systematic study, using bis-porphyrin compounds of the general structure in

(6) A referee questioned why α -methylstyrene is less reactive with malononitrile radicals than styrene. The electrophilic trichloromethyl radical reacts 4.2 times faster with α -methylstyrene than styrene at 80 °C (Kharasch, M. S.; Simon, E.; Nudenberg, W. *J. Org. Chem.* **1953**, *18*, 328). It is possible that the transition state for the malononitrile radical addition is located later on the reaction coordinate, so that steric effects are slightly larger.

(7) The kinetic method is described in the following: Giese, B.; Meixner, J. *Chem. Ber.* **1981**, *114*, 2138.

(8) In cyclization reactions, reversibility in additions of electrophilic radicals was observed in the absence of effective radical traps: Julia, M. *Pure Appl. Chem.* **1987**, *40*, 553.

(9) Calculations were carried out by using GAUSSIAN 90. For geometry optimizations and frequency calculations, the 6-31G* basis set was used with UHF wave functions. Zero point energies were scaled by 0.9. Post-SCF energies were determined by PMP3/6-31G*//UHF/6-31G* calculations with projection of the first spin contaminant as implemented by H. B. Schlegel (*J. Chem. Phys.* **1986**, *84*, 4530).

(10) Absolute energies calculated at various computational levels for transition state **9a**: UHF/6-31G*//UHF/6-31G*, -301.0464804; PMP3/6-31G*//UHF/6-31G*, -301.9897336. For **9b**: UHF/6-31G*//UHF/6-31G*, -301.0467342; PMP3/6-31G*//UHF/6-31G*, -301.9899853. For the malononitrile radical: UHF/6-31G*//UHF/6-31G*, -223.037874; PMP3/6-31G*//UHF/6-31G*, -223.6983886. For ethylene: HF/6-31G*//HF/6-31G*, -78.0317181; MP3/6-31G*//HF/6-31G*, -78.3053641. Zero point energies (in kcal/mol and scaled by 0.9): **9a**, 50.3; **9b**, 50.53; malononitrile radical, 17.9; ethylene, 30.9.

(1) (a) Marcus, R.; Sutin, N. *Biochim. Biophys. Acta* **1985**, *811*, 265–312. (b) A general review of recent work can be found in the following monograph: *Electron Transfer in Organic, Inorganic, and Biological Systems*; Advances in Chemistry 228; American Chemical Society: Washington, DC, 1991.

(2) Miller, J. R.; Beitz, J. *J. Chem. Phys.* **1981**, *74*, 6746–6753.

(3) (a) Cave, R.; Marcus, R.; Siders, P. *J. Phys. Chem.* **1986**, *90*, 1436–1444. (b) Ohta, K.; Closs, G.; Morokuma, K.; Green, N. *J. Am. Chem. Soc.* **1986**, *108*, 1319–1326.

(4) Closs, G.; Calcaterra, L.; Green, N.; Penfield, K.; Miller, J. R. *J. Phys. Chem.* **1986**, *90*, 3073.

(5) (a) Osuka, A.; Maruyama, N.; Mataga, N.; Asaki, T.; Yamazaki, I.; Tamdi, H. *J. Am. Chem. Soc.* **1990**, *112*, 4958. (b) Sessler, J.; Johnson, M.; Lin, T. Y.; Creager, S. *J. Am. Chem. Soc.* **1988**, *110*, 3659.

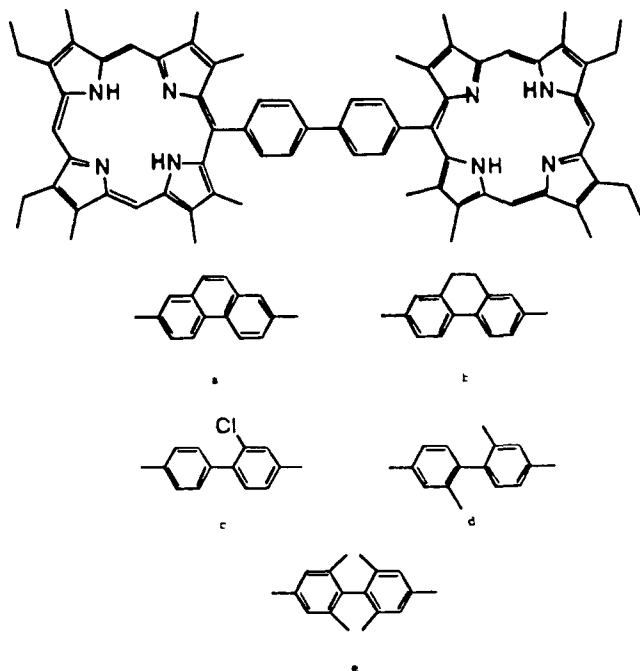


Figure 1. Structure of the angle dependent dimer series.

Figure 1. These systems were synthesized by the basic methodology described previously.⁶ They were purified by thin-layer chromatography and were characterized by ¹H NMR, UV/visible spectroscopy, and high-resolution mass spectrometry.^{6b}

The angle in these molecules between the mean porphyrin plane and the *meso*-phenyl group is rigidly constrained to 90° by the nonbonded contacts between the phenyl protons and the alkyl substituents on the flanking rings.⁷ Thus, the overall porphyrin-porphyrin dihedral angle is determined by the torsional angle, θ , at the biphenyl juncture. Many experimental methods have been employed in the measurement of the twist angle,⁸ including electronic absorption spectroscopy, ¹H NMR, ¹³C NMR, Raman spectroscopy, photoelectron spectroscopy, vapor-phase electron diffraction, and X-ray crystallography. For 2-substituted biphenyls, the nonbonded interactions dominate the potential, so that the twist angles measured by these various techniques agree closely⁸ and are essentially independent of substitution at the 4-position (e.g., CH₃ vs Br). We therefore believe that the angles determined for biphenyl will be equally applicable to porphyrinylbiphenyls. Since the rotational barriers around θ are rather high for biphenyl and its derivatives ($E_a > 30$ kcal/mol)⁸ and the reactions being studied are quite rapid ($k_{et} > 10^9$ s⁻¹), the angles that correspond to the lowest energy conformers of each bisporphyrin molecule should reasonably approximate the actual angles at the instant of electron transfer.

(6) (a) Heiler, D.; McLendon, G.; Rogalskyj, P. *J. Am. Chem. Soc.* **1987**, *109*, 604-607. (b) UV-vis spectra were similar for compounds A-E: maxima 405 ($\epsilon = 1 \times 10^5$), 505, 535, 569, 623. Mass spectral M for

	calcd	obsd
A	1076.6270	1076.6269
B	1078.6349	1078.6349
C	1051.5435	1051.5433
D	1080.6438	1080.6437
E	1138.844	1138.8445

A-E: Complete ¹H NMR spectra and synthetic details will be published separately.

(7) This is easily seen from molecular models and has been experimentally confirmed by crystallographic study of one such derivative (J. Sessler, personal communication).

(8) See, for example: (a) (¹H NMR) Bates, R.; Camou, F.; Kane, V.; Mistra, P.; Suvannachut, K.; White, J. *J. Org. Chem.* **1989**, *54*, 311. (b) (UV absorption) Suzuki, N. *Bull. Chem. Soc. Jpn.* **1959**, *32*, 1340. (c) (Raman) Schmid, E.; Brosa, B. *J. Chem. Phys.* **1972**, *56*, 6267. (d) (X-ray) Brock, C. *Acta Crystallogr., Sect. B* **1980**, *36*, 86.

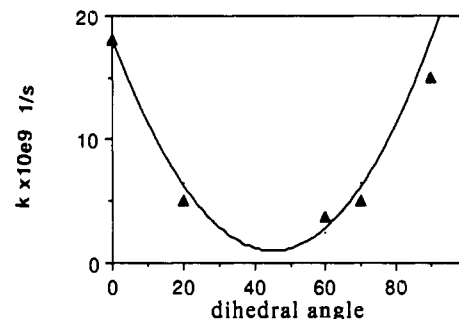


Figure 2. Plot of k_{et} vs dihedral angle for the angle dependent dimer series. The triangle gives the observed rates. The solid line is the line calculated from the tunneling matrix elements given in ref 3a, as described in the text.

In preliminary studies of these systems,⁶ we reported derivatives in which the electron donor is a free-base porphyrin in the singlet excited state and the electron acceptor is a low-spin Fe(III). For such derivatives, electron transfer is the primary deexcitation path for the excited states.^{5,6} Thus, by photoexciting these molecules, we can measure the corresponding electron transfer rates and how those rates depend on molecular orientation. In line with our earlier studies, these rates proved to be quite rapid. The rates have been determined by several independent methods: static fluorescence quenching, streak camera luminescence measurements, and picosecond pump-probe measurements which directly demonstrate the existence of electron-transfer products.

The results of the time-resolved studies are shown in Figure 2. Frankly, we were surprised by these results. Simple symmetry arguments had suggested that the rate at 90° would be much slower than that at 0°. This clearly is incorrect. Instead of the $\cos \theta$ dependence on rate which we anticipated, the results qualitatively follow a "cos 2 θ " function, with maxima at $\theta = 0^\circ$ and 90° and a minimum at 45°. Interestingly, this dependence was anticipated by a theory for bis-porphyrin systems developed by Cave, Marcus, and Siders.^{3a} Their simplified model focuses on the nodal structure of the porphyrin. When this complex nodal structure is taken into account, the dependence of rate on angle may follow a linear combination of $\sin \theta$ and $\cos \theta$, corresponding essentially to symmetric or antisymmetric wave function combinations. (The reader is advised to consult the original reference for details.)

In Figure 2, we have taken the values of $|V_{ab}|$ calculated by Cave et al.,^{3a} squared these (recall $k_{et} \propto |V_{ab}|^2$), and "normalized" the results to $\theta = 0^\circ$ in order to calculate the *predicted* dependence of rate on angle. The resulting prediction is given by the solid curve in Figure 2. The correspondence between theory and experiment is striking, suggesting that the simple theory of Cave et al.^{3a} may contain most of the key features of the dependence of rate on angle, at least for this porphyrin system. However, the theory of Cave, Marcus, and Siders was derived by assuming a simple "through space" coupling, with no electronic coupling through bridging atoms. For the present molecules, interaction through the bonding biphenyl seems quite likely. However, Gerhard Closs has pointed out (personal communication) that an analogous symmetry argument follows for coupling through biphenyl.

The porphyrin π orbitals are antisymmetric with respect to the porphyrin plane. Since, as noted above, the (bi)phenyl group is locked at 90° with respect to the porphyrin plane, the only ways to obtain π overlap between the phenyl bridge and the porphyrin must involve antisymmetric combinations of the biphenyl. Rotating from 0° and 90°, the bonding combination becomes antibonding, and vice versa, resulting in similar overlap at 0° and 90° with $|H_{AB}| \approx 0$ at 45°. Since this is basically a group theoretic argument, the same result will be obtained from any wave functions with two nodes along the long axis. In either case, it should be realized that it is the π orbital *symmetries* that are the key to the angular dependence. Thus, compounds with different nodal structures may be expected to exhibit a markedly different

angular dependence for electron transfer. If so, a quite different pattern of reactivity might be anticipated for systems with different nodal structures. For example, porphyrin radicals have different nodal planes than do the corresponding excited-state systems. We are currently designing experiments to test the effects of such electron redistribution in an intramolecular electron transfer rate.

In summary, we have prepared a series of bis-porphyrin molecules in which the angle between the donor and acceptor porphyrins is systematically varied. In these molecules, the intramolecular electron transfer rate varies by over 1 order of magnitude as the angle changes. This variance is anticipated by symmetry arguments which focus on the nodal properties of the molecules.³

Acknowledgment. We are grateful to R. Marcus, G. Closs, P. Siders, J. R. Miller, J. Sessler, and C. Chang for helpful discussions throughout the work. Support was provided by the National Science Foundation and the NIH (GM33881). Mass spectra were obtained at the MCMS.

Revised Assignment of Energy Storage in the Primary Photochemical Event in Bacteriorhodopsin

Robert R. Birge,* Thomas M. Cooper, Albert F. Lawrence, Mark B. Masthay, Chian-Fan Zhang, and Raphael Zidovetzki

Department of Chemistry and
Center for Molecular Electronics
Syracuse University, Syracuse, New York 13244

Received January 7, 1991

Bacteriorhodopsin is the light-transducing protein in the purple membrane of *Halobacterium halobium*.¹⁻⁵ Irradiation of the light-adapted form (bR) initiates a photocycle that pumps protons across the membrane. An accurate assignment of the energy storage associated with the primary event of bR is important to an understanding of the molecular mechanism and the stoichiometry of proton pumping.⁴⁻⁶ Previous photocalorimetric studies have concluded that ~ 16 kcal mol⁻¹ is stored in the K photoproduct, an energy sufficient to pump two protons per photocycle.⁶⁻⁸ However, this enthalpy (ΔH_{12}) was assigned assuming that the forward (Φ_1) and reverse (Φ_2) quantum yields associated with the bR \rightleftharpoons K photoreaction are $\Phi_1 = 0.33$ and $\Phi_2 = 0.67$.⁹ More recent investigations indicate that the above quantum yield values are significantly underestimated.¹⁰⁻¹⁵ Recently Govindjee et al.¹³ and Balashov et al.¹⁴ reported temperature-independent quantum yields of $\Phi_1 = 0.65 \pm 0.05$ and $\Phi_2 = 0.95 \pm 0.05$. The significant revisions in Φ_1 and Φ_2 have significant implications with respect to the energy storage, and this recognition prompted our reevaluation of the photocalorimetry

- (1) Oesterhelt, D.; Stoekenius, W. *Nature (London), New Biol.* **1971**, *233*, 149-152.
- (2) Oesterhelt, D.; Schuhmann, L. *FEBS Lett.* **1974**, *44*, 262-265.
- (3) Stoekenius, W.; Bogomolni, R. *Annu. Rev. Biochem.* **1982**, *52*, 587-616.
- (4) Lanyi, J. K. In *Bacteriorhodopsin and related light-energy converters*; Ernster, L., Ed.; North Holland: Amsterdam, 1984; pp 315-350.
- (5) Birge, R. R. *Biochim. Biophys. Acta* **1990**, *1016*, 293-327.
- (6) Birge, R. R.; Cooper, T. M.; Lawrence, A. F.; Masthay, M. B.; Vasilakis, C.; Zhang, C. F.; Zidovetzki, R. *J. Am. Chem. Soc.* **1989**, *111*, 4063-4074.
- (7) Birge, R. R.; Cooper, T. M. *Biophys. J.* **1983**, *42*, 61-69.
- (8) Cooper, T. M.; Schmidt, H. H.; Murray, L. P.; Birge, R. R. *Rev. Sci. Instrum.* **1984**, *55*, 896-904.
- (9) Becher, B.; Ebrey, T. C. *Biophys. J.* **1977**, *17*, 185-191.
- (10) Polland, H. J.; Franz, M. A.; Zinth, W.; Kaiser, W.; Kolling, E.; Oesterhelt, D. *Biophys. J.* **1986**, *49*, 651-662.
- (11) Oesterhelt, D.; Hegemann, P.; Tittor, J. *EMBO J.* **1985**, *4*, 2351-2356.
- (12) Schneider, G.; Diller, R.; Stockburger, M. *Chem. Phys.* **1989**, *131*, 17-29.
- (13) Govindjee, R.; Balashov, S. P.; Ebrey, T. G. *Biophys. J.* **1990**, *58*, 597-608.
- (14) Balashov, S. P.; Imasheva, E. S.; Govindjee, R.; Ebrey, T. G. *Biophys. J.*, in press.
- (15) Tittor, J.; Oesterhelt, D. *FEBS Lett.* **1990**, *263*, 269-273.

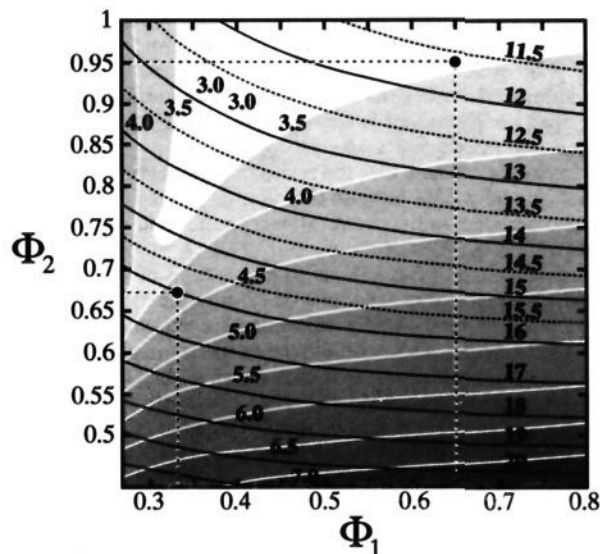


Figure 1. Enthalpy contour plot of ΔH_{12} as a function of the forward (Φ_1) and reverse (Φ_2) quantum yields associated with the photochemical interconversion of bR and K at 77 K based on experimental data from refs 6 and 7. The black contours indicate the ΔH_{12} values (enthalpies above contours on right). The white lines represent the error contours (ΔH_{12} standard deviations in gray on contours). The black dot on the left indicates the previously assigned value of energy storage ($\Delta H_{12} \approx 16$ kcal mol⁻¹; $\Phi_1 = 0.33$, $\Phi_2 = 0.67$). The black dot at upper right indicates the revised value of energy storage ($\Delta H_{12} = 11.6 \pm 3.4$ kcal mol⁻¹; $\Phi_1 = 0.65$, $\Phi_2 = 0.95$) (see text).

data. On the basis of the revised quantum yield assignments, the K photoproduct stores only 11.6 ± 3.4 kcal mol⁻¹. As noted below, the revised value of ΔH_{12} precludes a proton/photocycle stoichiometry larger than 1.

Weighted least-squares regression is carried out on the photocalorimetric data measured previously.^{6,7} The three experiments described in refs 6 and 7 generate a set of three equations:

$$\{0.907 \pm 0.021\} = \{\alpha_{565}^{>620}(1 - \Phi_1 \Delta H_{12}/50.6) + (1 - \alpha_{565}^{>620})(1 + \Phi_2 \Delta H_{12}/50.6)\} \quad (1)$$

$$\{1.294 \pm 0.033\} = \{\alpha_{699}^{500}(1 - \Phi_1 \Delta H_{12}/40.9) + (1 - \alpha_{699}^{500})(1 + \Phi_2 \Delta H_{12}/40.9)\} \quad (2)$$

$$\{1.201 \pm 0.024\} = \{\alpha_{643}^{500}(1 - \Phi_1 \Delta H_{12}/44.5) + (1 - \alpha_{643}^{500})(1 + \Phi_2 \Delta H_{12}/44.5)\} \quad (3)$$

where numbers in italics are in kcal mol⁻¹. Values for the three photochemical partition functions $\alpha_{565}^{>620}$, α_{699}^{500} , and α_{643}^{500} are dependent upon Φ_1 and Φ_2 and are assigned on the basis of the spectroscopic data of ref 6. The three equations are not truly independent,⁶ and a least-squares regression analysis can generate best fit values for only two variables as a function of one of the three variables Φ_1 , Φ_2 , and ΔH_{12} . In our previous studies, we arbitrarily chose Φ_1 to be the independent variable and assigned Φ_2 and ΔH_{12} as a function of Φ_1 . However, when values of Φ_1 exceed ~ 0.5 , the regression analysis incorrectly predicts values of Φ_2 that exceed unity (e.g., Table III of ref 6). This problem suggests that least-squares regression, in the absence of additional constraints, cannot provide an accurate assignment of ΔH_{12} for values of Φ_1 exceeding ~ 0.5 . We conclude further that our photocalorimetry data cannot assign Φ_1/Φ_2 with confidence. The problem can be corrected by treating both Φ_1 and Φ_2 as independent variables and carrying out a weighted least-squares regression to assign ΔH_{12} . The results are presented in Figure 1.

Evaluation of the results shown in Figure 1 indicates that the primary event stores $\Delta H_{12} = 11.6 \pm 3.4$ kcal mol⁻¹ ($\Phi_1 = 0.65$; $\Phi_2 = 0.95$), ~ 4.4 kcal mol⁻¹ less than our previous assignment of ~ 16 kcal mol⁻¹. A minimum of ~ 6 kcal mol⁻¹ of energy storage is required to pump a proton under ambient conditions.⁶ When entropic contributions are included, the revised value of